

The energy-dependent temporal variation of the ROSAT PSPC gain

M.A. Prieto¹, G. Hasinger^{1,2} and S.L. Snowden³

¹ Max-Planck-Inst. für extraterrestrische Physik, Germany
alm@rosat.mpe-garching.mpg.de

² Astrophysikalisches Institut Potsdam, Germany
ghasinger@aip.de

³ USRA/Goddard Space Flight Center
snowden@lheavx.gsfc.nasa.gov

Received August 29, 1995; accepted February 24, 1996

Abstract. — The existence of systematic spectral-fit residuals in *ROSAT* PSPC spectra, and their dependence on time, is by now a well established fact. This paper describes how those residuals may be related to second order variations of the gain of the PSPC as a function of energy and time. As a result, the energy scale used for the interpretation of PSPC spectra can be incorrect producing significant systematic effects, in particular at energies where the effective area of the instrument changes rapidly. A monotonic gain decay of $\sim 1\%$ per year is measured at 1 keV. A quantitative description of the PSPC gain-time variation as a function of energy is provided. The functional dependence of this variation is found to be well represented by a second order polynomial.

Key words: instrumentation: detectors — methods: data analysis — methods: observational — X-rays: general — space vehicles

1. Introduction

The Position Sensitive Proportional Counter, PSPC (Pfeffermann et al. 1986), on board *ROSAT* (Trümper 1983) is a multi-wire counter with an X-ray sensitive area of 8 cm diameter and covers the soft X-ray energy band from 0.1 to 2 keV. The spatial resolution of the *ROSAT* X-ray mirror assembly (XMA) plus PSPC is $\sim 25''$ at 1 keV and on-axis position (Hasinger et al. 1993). The energy resolution of the PSPC approaches that of a single wire proportional counter, about 40% FWHM at 1 keV over the entire sensitive area of the detector. The detector was calibrated extensively in the Panter long beam test facility at MPE/Neuried. A description of the various calibration corrections is in Hasinger & Snowden (1990). Monitoring of the performance of the detector during the operation life (1990 June – 1994 June) has been done using large and varied set of in-flight data. Information on the various re-calibration projects of the PSPC can be found in the *ROSAT* User's Handbook (Briel et al. 1995). This paper focuses on one particular monitoring project, namely, the

analysis of the on-axis variation of the gain¹ of the PSPC with time. Results of this analysis based on the extensive monitoring of the gain at different energies through the operational life of the PSPC are presented. The paper also provides a description of the various methods used in the analysis, which could be of interest for current and future X-ray missions. Previous results to the final ones presented here are in Prieto et al. (1994).

For a perfect proportional counter, the gain only depends on the potential difference between anode and cathode, the cathode wire diameter, and on the counter gas composition and density. In practice, the detector gain changes slowly due to spatial variations at the face of the detector and temporal variations from changes in the counter gas composition, high voltage, pressure, and temperature. The PSPC “nominal gain” is the slope of a linear relationship between PSPC pulse height and photon energy, measured by the peak channel of the on-board radioactive Al $K\alpha$ source (monochromatic $K\alpha$ line at 1.49 keV). There is a general trend of decreasing nominal gain throughout the *ROSAT* mission. Consequently, all PSPC data are corrected for temporal changes of the nominal

Send offprint requests to: M.A. Prieto

¹The PSPC gain is defined as the relationship between the pulse height and the energy of the photon event.

Table 1. Slope of gain change as a function of time

Energy [keV]	Slope Error [ch/yr]	Time-range ROSAT-day	Number spectra	Remarks
1.6	-0.03 0.15	250-1400	3	GX17+2 peak centroid
1.49*	-0.009 0.19	0-1400	10	On-board Al Line
0.90	-0.79 0.07	0-1200	8	N132 peak centroid
0.5249	-0.86 0.20	250-600	26	Geocoronal O K_{α} line
0.5249	-0.68 0.13	250-600	41	Geocoronal O K_{α} line (model)
0.30	-0.09 0.1	0-1000	35	C-edge of background spectrum
0.30	-0.61 0.14	0-1200	6	C-edge of 3C273
0.30	-0.69 0.1	0-1200	5	C-edge of Mkn 421
0.30	-0.69 0.07	0-1200	11	C-edge merging 3C273-Mkn 421
0.22	-0.25 0.03	0-1200	5	Mkn 421 fitting at C window
0.18	-0.18 0.03	300-1200	23	Meaty peak centroid
0.18	-0.56 0.33	0-1200	55	Centroid C-band background

*Assumed position for the Al line (see text)

gain by matching the mean peak channel of the Al K_{α} line to a fixed channel number, ~ 150 (Briel et al. 1989).

PSPC monitoring of the supernova remnant N132D has, however, revealed a monotonic shift of the peak of its energy distribution towards lower energies as a function of time. By the end of 1993, this shift amounted to 3% of the value of 0.9 keV measured at the beginning of the mission.

The study of this temporal gain variation has been extended to other energies through the analysis of a large sample of spectra from different sources. PSPC observations of the calibration sources N132D and the WFC-discovered white dwarf “Meaty” (RE J1629+780, Cooke et al. 1992) have been used for this purpose. In addition, the centroid positions of the geocoronal oxygen line and the nominal 1/4 keV band pulse-height distributions, both extracted from the background spectra of many pointed observations, have been examined as well. All of these sources present the advantage of having been monitored during the entire mission. In addition, because of their physical nature, they present characteristic features in their respective spectral distributions which are expected to lie at the same energy channel (although the 1/4 keV band distribution exhibits some variation with pointing direction, a large sample tends to average this out). Furthermore, some of them are characterised by a strong peak-dominant distribution at their respective mean energy (indicated in Table 1), thus becoming reasonably monochromatic for the PSPC.

To complement our calibration dataset, we have also analysed the fall-off of the high-energy side of the 1/4 keV band peak (caused by the carbon K_{α} absorption edge in the PSPC entrance window). The carbon edge (C-edge) of the PSPC presents a sharp break in the response at 0.284 keV, a feature that can be used in unabsorbed (by the ISM) PSPC spectra for monitoring gain variations at about that energy. For this purpose, we have used a large sample of PSPC background spectra selected among those *ROSAT* days having a minimum solar contamination. The

same spectral position was checked independently by using all available PSPC spectra from the radio source 3C273 and the BL Lac object Mkn 421. Despite these two sources being variable, the fact they are strong X-ray emitters showing a broad band featureless continuum across the PSPC energy range makes them suitable for the measurement of the C-edge position.

In the high-energy range of the PSPC, > 1 keV, we have used the spectrum of the low mass X-ray binary GX17+2. This source is absorbed through a hydrogen column density of $\sim 2 \cdot 10^{22} \text{ cm}^{-2}$ and together with the rapid drop in the XRT mirror reflectivity above ~ 1.49 keV causes the observed peak energy of the source to lie at roughly the same position despite the known spectral variations of the source. Time variations of that peak position have then been used for determining the gain-shift effect in the 1.4 – 1.8 keV range. Independently, several checks on the position of the on-board Al K_{α} source at 1.49 keV have been made.

Finally, the Mkn 421 dataset was used to validate our gain-shift predictions in the PSPC carbon-window. The residuals of the spectral fit in the 0.1 – 0.4 keV range were minimized by scaling the response matrix.

For comparative purposes, typical spectra of some of the sources used in this work are shown in Fig. 1.

2. N132D and Meaty dataset

The determination of the effective mean energies for the N132D and Meaty data sets has been done in the following manner. A total of 8 N132D and 23 Meaty PSPC observations spread in time from near the beginning of the mission (1991 June) until the end of 1993 have been analysed. All spectra have been rebinned into the standard SASS (the standard data processing software, Voges 1992) 34 energy bins, with unbinned channels 1 through 11 excluded from

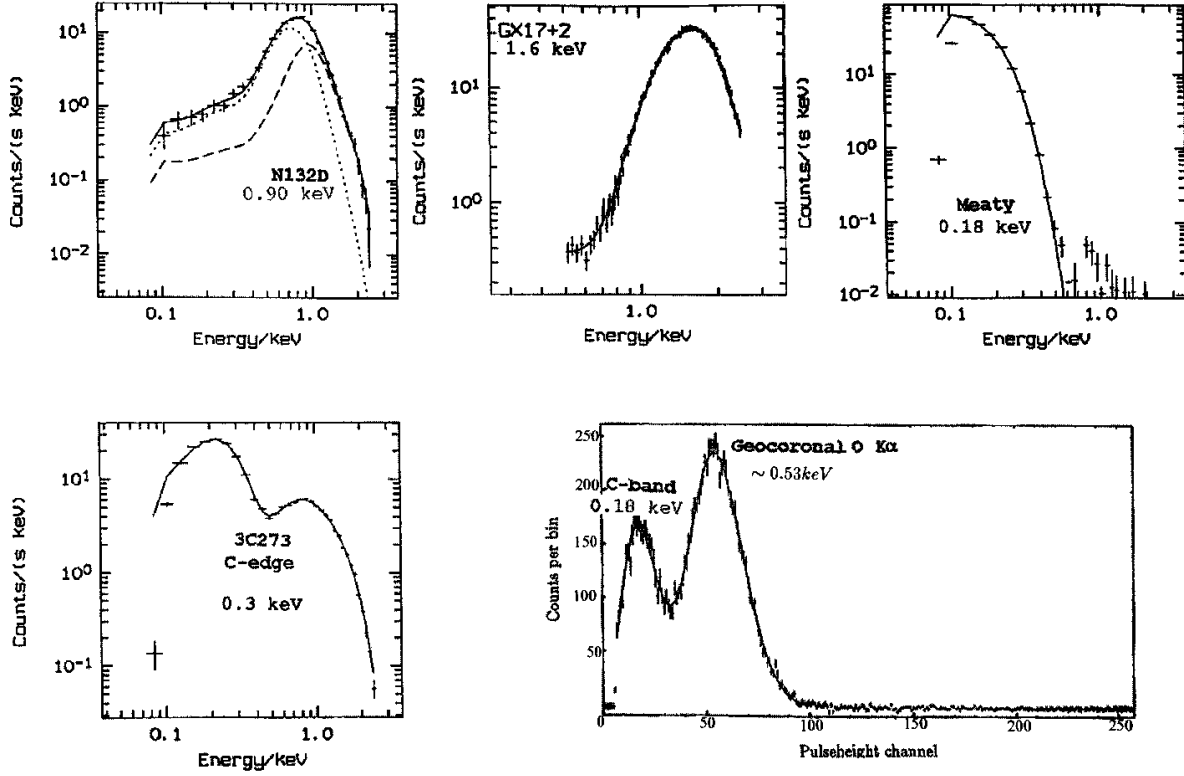


Fig. 1. PSPC spectra of different calibration sources with reference energies indicated. Best-fit models curves are overlaid: a) the supernova remnant N132D, fitted with a two temperature Raymond-Smith thermal plasma model; b) the Galactic source GX17+2 fitted with a power law; bf c) the white dwarf Meaty fitted with a single black-body; d) the quasar 3C273 fitted with a broken power law; e) a PSPC solar background spectrum, the peak at 0.18 keV is from the Thomson scattered solar component, the peak at about 0.53 keV corresponds with the geocoronal O K α line

the analysis. The mean energy, $\langle E \rangle$, and associated error, $\Delta \langle E \rangle$, were defined as follows:

$$\langle E \rangle = \frac{\sum_i [f_i(x) e_i(x)]}{\sum_i f_i(x)}$$

$$\Delta \langle E \rangle = \sqrt{\sum_i \left[\frac{e_i(x) - \langle E \rangle}{\sum_i f_i(x)} \Delta f_i(x) \right]^2}$$

$e_i(x)$: associated energy bin

$f_i(x)$: is the count rate per energy bin

The sum extends over the energy range 0.4 – 1.5 keV for N132D and over 0.12–0.5 keV for Meaty. Both enclose their respective $\langle E \rangle$ reference value, determined at the beginning of the mission, of 0.9 keV for N132D and 0.18 keV for Meaty. Note that the determination of the mean energy is independent of any physical model used to fit the data.

Over the time period considered, a monotonic energy shift, relative to respective values measured at the beginning of the mission, to lower energies was observed in both sources. Figure 2 shows this gain behaviour as a function of time for N132D. The gain decay has been characterised

in terms of a linear trend, and the corresponding gain-change rate has been derived accordingly. Table 1 gives the gain-change rate and associated errors for N132D and Meaty as derived from a linear χ^2 -fit to the data. The resulting linear fit for the N132D case is overlaid in Fig. 2.

3. Solar background dataset

The position of the oxygen K α line and the centroid of the PSPC 1/4 keV band distribution from the geocoronal background were derived from selected highly solar-contaminated background spectra. Series of background spectra are generated by SASS for each day of ROSAT PSPC observations. SASS provides time-consecutive background spectra corresponding to different positions of the satellite in its orbit while a fixed position on the sky is observed. For such a set of background spectra, the Galactic plus cosmic X-ray background component is always constant for a fixed pointing direction and the only expected variations in the background spectra are due to the solar contamination variation along the orbit (see Snowden & Freyberg 1993), plus possible long-term enhancements

(although there are occasional short-term contamination episodes as well; see Snowden et al. 1994).

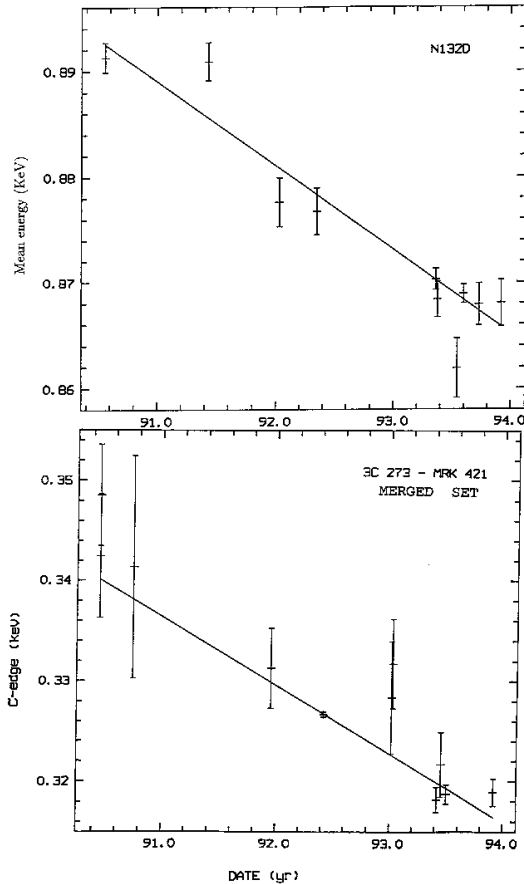


Fig. 2. Gain decay versus time: **a)** shift in the energy distribution peak of N132D; **b)** shift in the C-edge position as derived from the 3C273/Mkn 421 merged dataset

The solar contribution to the PSPC background light curve consists of two strong components: Thomson-scattered solar X-rays peaking at about 0.18 keV (after through the PSPC response) and a monochromatic geocoronal oxygen $K\alpha$ line at 0.5249 keV (see Fig. 1e). An accurate determination of the centroid position of these two components has been done on Galactic + Cosmic-background subtracted spectra. Accordingly, *ROSAT* days with relatively high solar contamination were selected. Figure 3 shows the light curve for a typical, high solar-contaminated *ROSAT* day; each point in the plot is the integrated PSPC count rate of the total background for 100 sec exposure, extracted from the outer ring of the PSPC field-of-view ($31' - 59'$ off-axis angle). The gaps in the figure correspond to those time periods in the orbit when the PSPC was turned off (due to passage through Earth's particle belts and South Atlantic Anomaly, SAA, or for slewing between targets). Between the gaps, each of the background slots contain coverage from a fixed position on the sky. From each of them, an average so-

lar/geocoronal contamination X-ray spectrum was extracted. This was done by subtracting an average spectrum of the low points in each slot from the corresponding one obtained from the highest points. To improve the statistics, the residual-contamination spectra were averaged to obtain a single solar/geocoronal background spectrum (see Fig. 1e) for each selected day.

Depending on the strength of the O $K\alpha$ line for each *ROSAT* day, the solar spectrum was used for determining either the centroid position of that line or, alternatively, the centroid position of the 1/4 keV band spectrum. In all cases, the spectrum was fit by a combination of two Prescott functions. The respective centroid positions and associated errors were derived from the resultant fits. As in the case of N132D and Meaty, they show a monotonic shift towards lower energies as a function of time that can be characterised in terms of a linear trend. Error-weighted linear regression was applied to the respective gain decay at 0.18 keV and 0.53 keV with the resulting gain-change rates given in Table 1. Note that because of the diminishing solar activity starting from 1992 March (as the solar maximum was passed), only few spectra showing significant geocoronal $K\alpha$ line could be used in the period 1992 March to the end of 1993. The gain change-rate derived from this dataset is thus more uncertain, yet it is in fairly good agreement with the result obtained from a different method described below.

A more rigorous evaluation for the O $K\alpha$ line effective energies has been done using deep PSPC pointed observations. 41 spectra collected from 1990 July to 1993 October were examined, the geocoronal X-ray spectrum extracted, and the energy of the O $K\alpha$ line fitted together with a full model of the underlying solar spectrum, folded through the detector response matrix (DRM 36). The assumed emission temperature for the solar X-rays was allowed to vary as an uninteresting parameter to achieve the best fit. The fitted energy of the O $K\alpha$ line shows a systematic decrease over the time interval covered by the data, which can as well be represented by a linear decay. The result is within the errors consistent with the decay measured with the former method on a different set of background spectra (see Table 1) and has a higher statistical accuracy due to the larger baseline of *ROSAT* days that could effectively be used.

4. Solar-uncontaminated PSPC background and 3C273 dataset

The transmission of the plastic window of the PSPC has a sharp break at 0.284 keV, produced by the C $K\alpha$ absorption edge. Temporal gain variations around that energy have been monitored through the analysis of a large sample of PSPC background spectra, in this case selected among those *ROSAT* days having a minimum solar contamination. Essentially, those days with background spectra lacking the O $K\alpha$ line were selected, then all

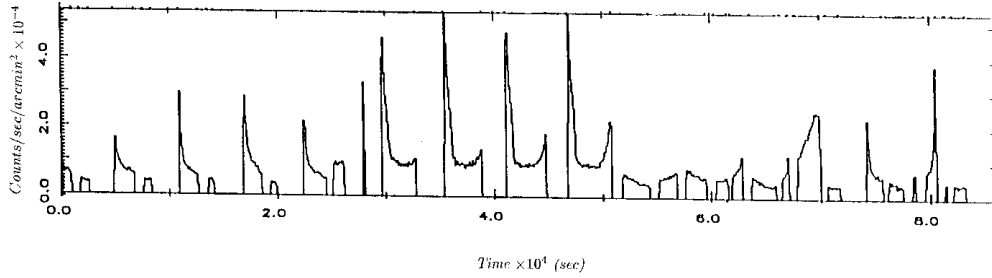


Fig. 3. PSPC background count rate for one *ROSAT* observation day. The background data are extracted from a ring away from the central source ($31' - 57'$ off-axis), bright additional sources falling in the ring were removed

background spectra from each selected day were averaged separately. A total of 35 average spectra covering the period from 1990 June to the end of 1993 were finally generated. In addition to these data, we used all available PSPC spectra from the radio source 3C273 for the same purpose. A total of six spectra covering the period from 1990 June to 1993 June were examined. Although 3C273 is variable, the fact that it is a strong X-ray source showing a broad band featureless continuum across the PSPC windows (see Fig. 1d) makes it suitable for determination of the C-edge position.

The follow-up procedure was the same for both datasets. The position of the carbon edge was defined as that at which the intensity of the spectrum within the carbon window is reduced to half the maximum (peak) value. We derived an accurate determination of that position as follows. First, the maximum intensity in the carbon band was found by examining the six channels nearest the peak. The value of half this maximum was determined and a value for its channel position at the high-energy side of the $1/4$ keV peak estimated. Next, a linear regression to this region of the spectrum and within the four adjacent channels around the estimated value provided the true half maximum.

We found the error associated with that position to be dominated by the uncertainties in determining the maximum value in the carbon window region. Over the time period covered by this analysis, the position of the C-edge shows a systematic shift to lower energies that can again be well be represented by a linear decay.

Two independent gain-change rates were derived after applying the linear fits to each dataset. The slope of the linear regression to the background dataset was ~ 0.086 ch/yr, and to the 3C273 spectra was ~ 0.614 ch/yr (see Table 1). There is a clear discrepancy between the two estimates, larger than the reported errors, which becomes more accentuated when compared with the 0.69 ch/yr gain-change rate derived, using the same method, from the Mkn 421 dataset (see Sect. 6). The discrepancy is probably due to the fact that the background dataset is mainly the contribution of the various non-cosmic background components, which vary with time, and that from galac-

tic and extragalactic components, whose shape varies with the observation direction. The detection of any shift in the gain from this dataset may be smeared out by those variations, hence the almost compatible with zero gain-rate derived from these observations.

5. GX17+2 dataset

GX17+2 is a low mass X-ray binary source showing a strong, hard spectrum in the PSPC band. The mean-energy peak position of its spectrum falls at about 1.6 keV. Even though it has known spectral variability, its peak energy position is expected to lie roughly at the same energy channel: at lower energies, the spectrum is heavily absorbed by $N_{\text{H}} \sim 2 \cdot 10^{22} \text{ cm}^{-2}$; at higher energies, the influence of any spectral variability on the mean energy is minimized by the rapid drop in the XRT mirror reflectivity above 1.5 keV.

Monitoring of the gain-shift effect in GX17+2 was carried out by applying the same procedure as described for N132D and Meaty (see Sect. 2). The GX17+2 dataset includes only three spectra distributed through the mission: a survey spectrum and two pointed observations, globally they cover the period 1991 January (*ROSAT* survey) - 1994 March. An accurate determination of the mean-energy peak and error was obtained through the formulae described in Sect. 1, the energy range expanding in this case over $1.4 - 1.8$ keV range.

The linear regression to the peak position versus time yields a slope of -0.025 ch/yr, in very good agreement with the expected constancy of the Al $K\alpha$ line position at 1.49 keV (see Fig. 5).

6. Mkn 421 dataset

A total of 5 spectra covering the period from 1991 January (survey data) to the end of 1993 have been analysed. This dataset was used for two different purposes: first, to determine the position of the C-edge and second, to validate our gain-shift predictions at about 0.2 keV. The position of the C-edge was determined following the same procedure as described in the previous section. The

derived gain-change rate from this dataset is ~ 0.69 ch/yr, in very good agreement with the value derived from the 3C273 dataset. This agreement accentuates the obvious discrepancy with the value derived from the background spectra (see the end of Sect. 4). As a final value, we used that derived from the linear fitting to the merged 3C273 - Mkn 421 data set. Figure 2b shows the gain-shift values from the two respective dataset and the global linear fitting. The resulting slope of the curve is 0.685 ch/yr (see Table 1).

The PSPC spectrum of Mkn 421 obtained in May 1992 was used to fudge the PSPC response matrix. We used this fact to check out whether our gain shift predictions were consistent with those derived after optimal spectral fitting to the Mkn 421 dataset. For each of the Mkn 421 spectra, the optimal fitting in the 0.1 – 0.4 keV range was achieved by shifting the current PSPC matrix by small, consecutive values in the reference nominal value of the gain and the residuals were minimized. Proper gain-shift and associated one sigma error were determined from the χ^2 distribution generated from the series of fits. For our purposes and for sake of clarity, no modifications to the slope of the gain were applied, which was kept to its nominal value. Since the gain shift is different depending on energy, the complete Mkn 421 spectrum was not fitted at once, only the spectral region falling inside the carbon window was used.

The Mkn 421 spectrum in the carbon window strongly peaks at about 0.22 keV. Therefore, we expect shifts in the gain to be dominated by those occurring at about this energy. Figure 4 shows the optimal gain shift applied to the different Mkn 421 spectra, i.e., that corresponding to the minimum value of our χ^2 distribution. Since the May 92 spectrum (middle of the plot) was the one used to tune the matrix, the corresponding gain-shift is expected to be small, as derived. Note that the small error bars associated with this measurement are due to the large exposure time for this particular observation.

As it can be seen in Fig. 4, the *ROSAT* survey spectrum requires a positive shift in the gain whereas the spectra taken in 1993 require a gradually more negative gain-shift. The slope of a linear fit to the data, i.e. the gain-change rate, is -0.254 ch/yr and thus, consistent with what is expected at about 0.22 keV (see Fig. 5).

7. Calibration of spectra collected during 1994: End of PSPC life

1994 was the last year of PSPC operations (formally ended in 1994 September). During this year the instrument was occasionally on focus, mainly devoted to calibration observations.

During the time period covering 1994 end of March to July, a set of in-flight calibration observations were collected aimed at providing an end-of-life description of the PSPC detector. These observations were taken after a

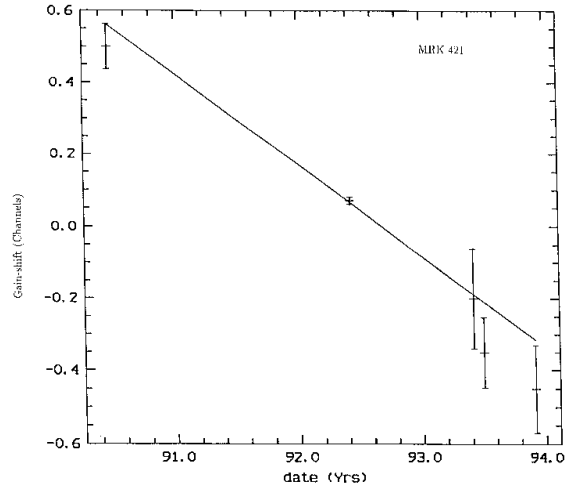


Fig. 4. Gain decay versus time at ~ 0.2 keV derived from the Mkn 421 dataset. The data point corresponding to 1992 May (middle) was extracted from the Mkn 421 spectrum used to fudge the PSPC matrix. Note that the gain associated with the other spectra are relative to the 1992 May spectrum

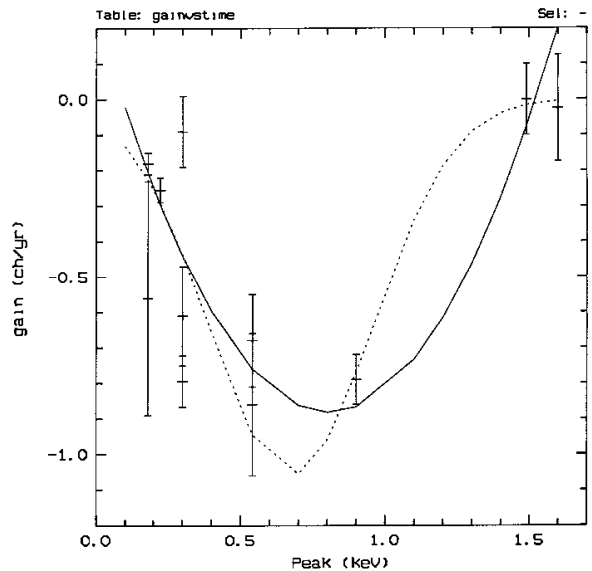


Fig. 5. The rate of the gain change in the *ROSAT* PSPC as a function of energy. Calibration sources include the Meaty white dwarf, the peak of the *C*-band background (0.18 keV) and Mkn 421 (0.2 keV), the *C*-edge from 3C273, Mkn 421, and X-ray background spectra (0.28 keV), the geocoronal O $K\alpha$ line (~ 0.5249 keV), the SNR N132D (0.90 keV) and the Galactic source GX17+2. Two possible fittings to the observed trend are overlaid: a second order polynomial (—) and a Gaussian function (..). The point having the smaller gain-change rate at 0.3 keV has been excluded from the fit (see text)

period of two and a half months in which the PSPC was switched off. After the re-activation, the PSPC showed a systematic increase in the gain that clearly departed from the usual smooth decay it was showing during 1993. The results from the analysis of N132D, Meaty and 3C273 data taken in particular during the June - July 94 period were found largely divergent from those derived from the previous years of continuous PSPC operation. Given the anomalous PSPC gain behaviour, these later data have not been included in the present analysis as they were considered not representative of the overall PSPC life. Thus, our general results should be regarded as representatives of the PSPC life time, starting with the beginning of the *ROSAT* mission, June 1990, until the end of 1993.

8. Conclusions

The change rate of the PSPC gain with time and energy has been evaluated. The time period analysed covers the PSPC nominal time life, which extends from beginning of the *ROSAT* mission, June 1990, till the end of 1993 that corresponds with the end of PSPC science observations.

Figure 5 shows the resulting gain-change rates as a function of energy as derived from the different sources used in this analysis. The assumed position of the on-board Al $K\alpha$ line is also shown. The position of this line was checked via a fit to the calibration data folded through the detector response matrix. About 10 Al $K\alpha$ spectra chosen to be uniformly spread along the mission were selected for that purpose. Only photons from the central inner ring of the PSPC were used to generate the Al $K\alpha$ spectra. The fits show that the position of the Al $K\alpha$ line has remained, within the errors, stable along the mission, no relative variations with respect to the position measured at the beginning of the mission are detected at that energy, confirming the validity of the first-order gain correction.

Figure 5 shows a clear increase of the gain change rate with energy out to ~ 1 keV followed by a decrease to the nominal values at 1.5 keV, thus reflecting a temporal non-linearity in the energy scale. The observed trend has been approximated by two different functions: a second order polynomial and a gaussian function. In the fit, the discrepant gain-change rate at the C-edge position, as deduced from the background dataset (see former section) has been excluded. Both fits are overlaid in Fig. 5, the second order polynomial giving at first glance a better representation of the observed behaviour.

We would like to remark on some important points related to the used methodology and derived results. These are the following: 1) the various measurements of the gain change rate are derived from independent datasets; 2)

within each dataset, *relative* time-variations of the PSPC gain at a given energy are determined, no absolute zero value of the gain scale at each energy is considered; 3) in each dataset, the gain-shift is determined by comparing spectra of the same source and almost same spatial location on the detector. All point sources considered are on axis position, excluding when survey data has been considered (see below); diffuse radiations have always been accumulated from the same region in the detector. In consequence, spatial variations of the gain across the detector are expected to have a minor effect on the derived gain-rates. In the case of survey data, the position of the source on the PSPC changes with the continuous slew of the satellite; however, as the *ROSAT* survey has been produced at the beginning of the mission, we expect at this point no substantial variations of the gain across the face of the detector.

In an attempt to understand the observed gain decay, we have searched for a potential correlation with significant changes in the nominal gain, occurring as a result of ageing of the PSPC and changes in the high voltage setting. However, no clear relationship could be found.

A second important aspect in the PSPC calibration concerns the spatial stability of the gain across the face of the detector. We have been examining the complete set of Al $K\alpha$ in-flight observations, that cover the entire PSPC life, to verify the stability of the nominal gain correction over the PSPC field-of-view. Preliminary results are reported in Snowden et al. (1995) and the final results will be made available to the community in the near future.

Acknowledgements. We are thankful to A. Gruber and M. Klug for their work in the processing of part of the data discussed here during their stay at MPE doing a Semester Practicum through the Ludwigs-Maximilians University.

References

- Briel U., Burkert W., Pfeffermann E., 1989, SPIE 1159, 263
- Briel U., et al., 1995, The ROSAT User's Handbook, MPE
- Cooke B.A., et al., 1992, Nat 355, 61
- Hasinger G., Boese G., Predehl P., et al., 1993, Legacy 4
- Hasinger G., Snowden S., 1990, TN-ROS-MPE-ZA00/27
- Pfeffermann E., et al, 1986, SPIE 733, 519
- Prieto M.A., Hasinger G., Snowden S., 1994, TN-ROS-MPE-ZA00/32
- Snowden S.L., Freyberg M.J., 1993, ApJ 404, 403
- Snowden S.L., McCammon D., Burrows D.N., Mendenhall J.A., 1994, ApJ 424, 714
- Snowden S.L., Turner T.J., George I.M., Yusaf R., Predehl P., Prieto M.A., 1995, OGIP Calibration Memo CAL/ROS/95-003
- Trümper J., 1983, Adv. Space Res. 2, 241
- Voges W., 1992, Proc. ESA YSY-3 Conf., p. 9